*Annals of Biomedical Engineering*, Vol. 50, No. 7, July 2022 *(© 2022)* pp. 860–870
https://doi.org/10.1007/s10439-022-02961-w

*Original Article*

# The Effect of MIPS, Headform Condition, and Impact Orientation on Headform Kinematics Across a Range of Impact Speeds During Oblique Bicycle Helmet Impacts

STEPHANIE J. BONIN [1,2] ALYSSA L. DEMARCO,[3] and GUNTER P. SIEGMUND [1,4]

[1]MEA Forensic Engineers & Scientists, 23281 Vista Grande Drive, Laguna Hills, CA 92653, USA; [2]Biosystems and Ag. Engr., University of Kentucky, Lexington, KY, USA; [3]MEA Forensic Engineers & Scientists, Richmond, BC, Canada; and [4]School of Kinesiology, University of British Columbia, Vancouver, BC, Canada

*(Received 23 November 2021; accepted 28 March 2022; published online 19 April 2022)*

Associate Editor Megan L. Bland oversaw the review of this article.

**Abstract**—Bicycle helmets are designed to attenuate both the linear and rotational response of the head during an oblique impact. Here we sought to quantify how the effectiveness of one popular rotation-attenuating system (MIPS) varied across 3 test headform conditions (bare, covered in stockings, and hair), 3 oblique impact orientations, and 4 impact speeds. We conducted 72 freefall drop tests of a single helmet model with and without MIPS onto a 45° angled anvil and measured the peak linear (PLA) and angular acceleration (PAA) and computed the angular velocity change (PAV) and brain injury criterion (BrIC). Across all headform conditions, MIPS reduced PAA and PAV by 38.2 and 33.2% respectively during *X*-axis rotation, 47.4 and 38.1% respectively during *Y*-axis rotation, and 22.9 and 20.5% during a combined *ZY*-axis rotation. Across all impact orientations, PAA was reduced by 39% and PAV by 32.4% with the bare headform while adding stockings reduced PAA and PAV by 41.6 and 36% respectively and the hair condition reduced PAA and PAV by 30.2 and 24.4% respectively. In addition, our data reveal the importance of using consistent headform conditions when evaluating the effect of helmet systems designed to attenuate head rotations during oblique impacts.

**Keywords**—Oblique impact, Brain injury, Rotational.

## INTRODUCTION

During many cycling-related head impacts, the head strikes the ground at an oblique angle and experiences both linear and angular accelerations.[9,15,35,46] Linear head acceleration is associated with transient changes in intra-cranial pressure and focal-loading injuries such as skull fractures.[19,26,30,42] Angular head acceleration (and the resulting angular velocity change) is associated with shear deformation of brain tissue, which is the predominant mechanism of injury in vascular and diffuse axonal injuries (DAI),[17,32,45] and concussions,[21,24,36,40] all of which can occur in cyclist crashes.

The expanded polystyrene (EPS) liners in conventional bicycle helmets are designed to crush and crack during an impact, thereby distributing the impact force over a larger area of the skull, increasing the impact duration and reducing the peak linear acceleration experienced by the head. Conventional bicycle helmets can also reduce the head's angular acceleration, but they do so by reducing the impact force that generates a moment about the head's center of mass or some other center of rotation.[16,27] More recently, helmet-integrated systems that have been specifically designed to further reduce angular head kinematics are available to consumers.[4,6,8,20, 25,39] One example of these systems is the Multi-directional Impact Protection System (MIPS), a thin, low-friction plastic layer that is loosely tethered between the interior surface of the EPS liner and the wearer's head. During a non-centroidal impact, i.e., an impact with a force that has a circumferential component, slip between the MIPS liner and the helmet allows the helmet to rotate relative to the head and thus reduces the angular impulse applied to the head.[1]

Many prior studies have shown that MIPS reduces the peak angular headform kinematics during oblique impacts[5,6,8,39] Although these researchers have tested

Address correspondence to Stephanie J. Bonin, MEA Forensic Engineers & Scientists, 23281 Vista Grande Drive, Laguna Hills, CA 92653, USA. Electronic mail: stephanie.bonin@meaforensic.com

various helmets using different headforms (e.g., Hybrid III, National Operating Committee on Standards for Athletic Equipment (NOCSAE) with and without necks), impact locations (e.g., forehead, side), impact speeds (4.8 to 7.4 m/s), anvil angles (30° to 60° from horizontal) and drop conditions (e.g., drop rails vs. freefalls), less attention has been focused on the effect of the interface between the headform and the helmet or MIPS liner. Neither the Hybrid III headform nor the NOCSAE headform were designed to replicate the circumferential shear properties of the human scalp relative to the skull and various studies have shown that headform kinematics are influenced by the headform/helmet interface.[14,44,47] For instance, peak angular kinematics were reduced with a lower friction headform surface during an oblique helmeted impact[14] and with a porcine scalp attached to a Hybrid III headform.[44] Nylon stockings are often placed over a Hybrid III headform during helmet testing to reduce the friction between the headform and the helmet;[6,8] however, the kinematic response of this headform condition compared to a human scalp—with varying amounts and lengths of hair—in helmeted oblique impacts remains unknown.

Here we sought to quantify the effect of MIPS (present vs. absent) on peak headform kinematics for three headform conditions: bare vinyl-nitrile skin, two layers of stockings over the bare skin, and a human-hair wig for a range of impact speeds at three oblique impact orientations. We hypothesized that the reduction in peak angular headform kinematics for MIPS relative to a no-MIPS helmet ($\Delta_{MIPS}$) would vary with headform condition, impact orientation, and impact speed. In addition to this omnibus analysis, we also sought to address two specific questions. First, we wanted to understand if headform condition affects the angular kinematics without MIPS. We hypothesized that angular kinematics would be larger for the bare headform compared to a stocking or hair-covered headform. Second, we wanted to determine if hair behaved like a built-in anti-rotation system. Here we hypothesized that the reduction in peak angular kinematics from a MIPS helmet on a bare or stocking-covered headform would be different than a no-MIPS helmet on a headform with hair. We further hypothesized that adding a MIPS helmet to the hair or stocking condition would further reduce peak angular kinematics compared to the no-MIPS condition.

## METHODS

Specialized Echelon II helmets manufactured between 2019 and 2021 with MIPS (size L) were purchased from retail stores and websites. The Echelon II is a traditional-style vented bicycle helmet in the mid-price range with a polycarbonate micro shell, an EPS liner, a MIPS layer, and thin strips of comfort padding. The MIPS layer was removed, and the comfort padding was replaced over the EPS in half of the helmets to create a no-MIPS condition. Helmets were fit to a 50th percentile Hybrid III headform (4.72 kg, Humanetics, Farmington Hills, MI, USA) that was tested in three different conditions: bare (B), covered in two layers of nylon stockings (S), or covered with a human hair wig (H) (Fig. 1). The wig consisted of 30 cm long human hair (Eva & Co. Wigs, Vancouver, BC, CA) woven into a textured cap that adhered well to the headform's vinyl nitrile skin. The hair was gathered with an elastic at the occiput. The distance from the inferior surface of the helmet brow to the headform's Frankfort plane was 50.8 mm and the ring-fit system was tightened until slight resistance was met. The chinstrap was adjusted so that 2–3 fingers fit comfortably between the buckle and headform's chin, and low-density foam was then inserted into this space to prevent the tails of the straps from slapping the headform during the impact. The foam did not influence the chinstrap's position relative to the headform during testing and did not alter the headform's response.

The headform and helmet were inverted and placed on a U-shaped freefalling trolley (3.823 kg) that fell past a 45° anvil covered with 40-grit sandpaper. The anvil weighed 66 kg and was rigidly mounted to a steel plate (133 kg) which was fastened to an 800 kg concrete base poured into the floor. Three headform orientations were used (Fig. 2). For orientations 1 and 2, the $X$- and $Y$-axes of the headform were within $\pm$ 1° of horizontal when positioned on the trolley prior to impact. For orientation 3, the headform was rotated -65° about the $Y$-axis, i.e., facing downward, when positioned on the trolley prior to impact. To ensure consistent placement of the headform and helmet, an inertial measurement unit (MetaMotionR, MBIENTLAB, Inc, San Francisco, CA, USA) was mounted to the headform to display the headform's real-time orientation. In addition, to ensure consistent initial positions between matching MIPS and no-MIPS tests, an image of the initial headform position with a no-MIPS helmet was captured and then overlaid on a live image of the MIPS condition at 50% transparency (Fig. S1, Supplemental Materials).

Two helmets, one with MIPS and one without MIPS, were tested at each combination of three headform conditions (B, S, H), three impact orientations (1, 2, 3) and four impact speeds (4.2, 5.1, 6.2, and 7.2 m/s), for a total of 72 impacts. A cantilevered arm held the headform in place during the freefall and was automatically retracted prior to impact (Fig. 2). A

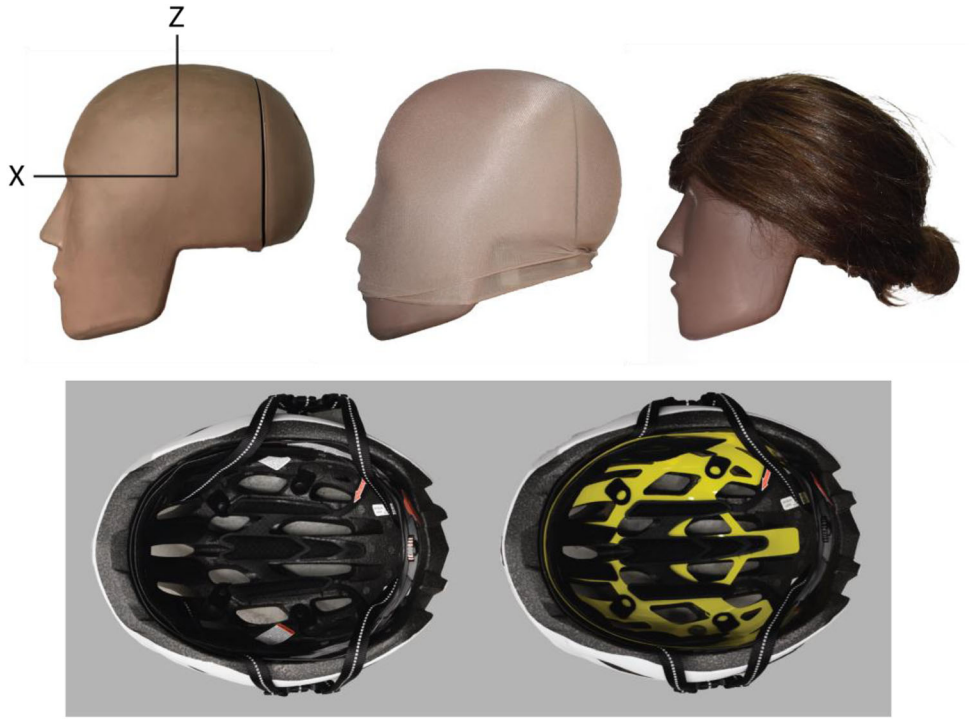


**FIGURE 1. The 50th-percentile male Hybrid III headform in the bare, stocking-covered, and human-hair wig-covered conditions and an internal view of the Specialized Echelon II helmet without MIPS (bottom left) and with MIPS (yellow layer, bottom right).**

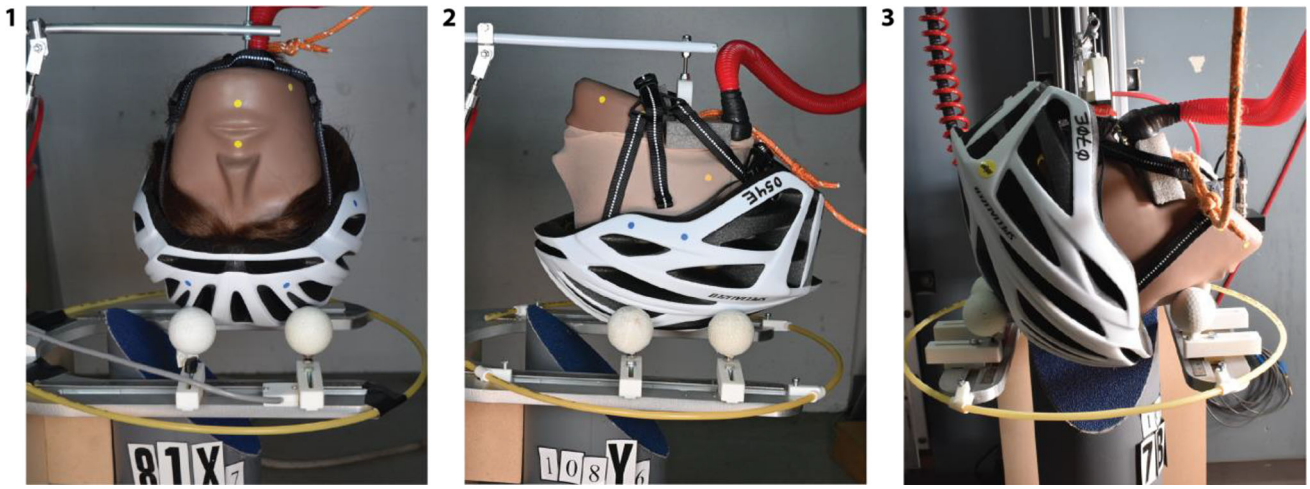


**FIGURE 2. Headform and helmet shown in orientation 1 (hair-covered), orientation 2, (stocking-covered) and orientation 3 (bare).**

slack tether attached to the headform prevented secondary impacts. Most helmets underwent two tests (maximum three tests), with the centers of the impact locations separated by at least 120 mm.[13]

Six degree-of-freedom headform kinematics were captured with a 3-2-2-2 accelerometer array (2000 g, TE Connectivity, Schaffhausen, Switzerland; $r_x$ = 56 mm, $r_y$ = 48 mm, $r_z$ = 81 mm) sampled at 50 kHz. All data channels conformed to SAE Channel Filter Class (CFC) 1000[37]. High-speed video was recorded at 1 kHz (Chronos 1.4, Krontech, Vancouver, BC, Canada). Angular acceleration was computed from all nine accelerometers[33] and angular velocity was calculated by integrating the components of the angular acceleration using the trapezoidal rule. These time-varying kinematic signals were then low-pass filtered at 300 Hz[31,37] before extracting the peak resultant angular acceleration (PAA) and peak resultant angular velocity change (PAV). The Brain Injury Criterion (BrIC) was then computed from the angular velocity signals.[41]

Although our hypotheses focused on peak angular kinematics, we also analyzed and reported the peak resultant linear acceleration (PLA), which was extracted directly from the three orthogonal accelerometers at the headform's center of mass and also filtered at 300 Hz. All post-processing was done using a customized MATLAB script (v2019b, MathWorks, Natick, MA).

Repeatability was evaluated with three impacts of MIPS and no-MIPS conditions at the 6.2 m/s impact speed using three combinations of impact orientation and headform condition: (a) orientation 1 and bare condition, (b) orientation 2 and hair condition, and (c) orientation 3 and stocking condition. The coefficient of variation (CoV) was calculated for impact speed and peak headform kinematics for each combination of conditions.

For each pair of helmets tested at the same impact condition, we first computed the reduction in each kinematic response due to MIPS ($\Delta_{MIPS}$), defined as the no-MIPS response minus the MIPS response, divided by the no-MIPS response, expressed as a percentage. We used a General Linear Model (GLM) to test our primary hypotheses that $\Delta_{MIPS}$ varies with headform conditions (B, S, H) and impact orientation (1, 2, 3), including speed as a co-variate. Separate models were run for PLA, PAA, PAV, and BrIC. We then used post-hoc Tukey–Kramer tests to assess differences between the headform conditions and impact orientations. These tests were performed at a significance level of $\alpha = 0.05$ using Minitab (v19, State College, PA, USA).

To evaluate our secondary hypotheses, we first normalized all peak kinematic data to the peak response obtained in the bare-no-MIPS headform condition at the same impact speed and orientation. This normalization procedure generated numbers less than one if the helmet-headform combination reduced the peak angular kinematics relative to the baseline condition (bare-no-MIPS). We then calculated the means and standard deviations of these normalized values for all helmet-headform combinations and tested whether they were significantly different from one (the normalized baseline condition). A one-sample Student's t-test was used to compare angular kinematics of the bare-no-MIPS condition to the no-MIPS-stocking and no-MIPS-hair conditions (specific question 1). A two-sample Student's t-test was used to compare angular kinematics of the MIPS-bare condition to no-MIPS and MIPS-hair conditions as well as the no-MIPS to MIPS conditions for both hair and stockings (specific question 2). These secondary tests were calculated in Microsoft Excel (v16.5, Redmond, WA) at a significance level of $\alpha = 0.05$.

## RESULTS

The means and standard deviations (SDs) of the four impact speeds were $4.12 \pm 0.05$ m/s, $5.13 \pm 0.06$ m/s, $6.24 \pm 0.04$ m/s, and $7.22 \pm 0.05$ m/s when pooled across the two helmet conditions, three headform conditions and three impact orientations (see Fig. S2, Supplemental Materials for example data). Across the 18 impacts used to assess repeatability, the impact speed was $6.23 \pm 0.04$ m/s (CoV = 0.58%). Within the six groups of tests used to assess repeatability of the peak kinematic responses, the CoVs for PLA were less than 3% and the CoVs for PAA and PAV were less than 8%, except for one condition with a MIPS helmet on the stocking headform in impact orientation 3, where the CoV was about 12%. (Table 1).

Three general patterns were visible in the peak kinematic data (Fig. 3): the first and most apparent pattern was that all three peak kinematic parameters increased with increasing impact speed; the second pattern was that the MIPS helmets (blue lines in Fig. 3) yielded lower peak angular kinematics than the no-MIPS helmets (red lines in Fig. 3); and the third pattern was that PLA was less sensitive to changes in the helmet and headform conditions than PAA and PAV.

Impact orientations 1 and 2 generated nearly pure *X*- and *Y*-axis headform rotations respectively, whereas orientation 3 produced a combined headform rotation, mostly about the *Y*- and *Z*-axes (Fig. S3, Supplemental Materials).

With respect to our primary hypotheses, the percent reduction due to MIPS ($\Delta_{MIPS}$) for the peak angular kinematics (PAA and PAV) varied significantly with both headform condition and impact orientation (Table 2). Post-hoc testing showed that $\Delta_{MIPS}$ was larger, i.e., MIPS was more effective, for the bare and stocking conditions than the hair condition. MIPS was more effective in reducing PAA and PAV for orientation 2, with maximum reductions of 47±13 and 38.10% respectively. BrIC exhibited a similar response to PAV, whereas PLA exhibited either small or no

**TABLE 1. Coefficient of Variation (CoV, in percent) for both helmet conditions at the three combinations of impact orientation and headform condition used to assess repeatability.**

| Orientation | Headform | Helmet | PLA | PAA | PAV |
|---|---|---|---|---|---|
| 1 | Bare | N | 1.09 | 7.63 | 3.94 |
| | | M | 0.62 | 5.43 | 1.06 |
| 2 | Hair | N | 2.04 | 5.40 | 1.18 |
| | | M | 2.68 | 4.85 | 4.32 |
| 3 | Stocking | N | 1.68 | 6.32 | 5.52 |
| | | M | 1.78 | 12.37 | 6.53 |

*N* no-MIPS, *M* MIPS.

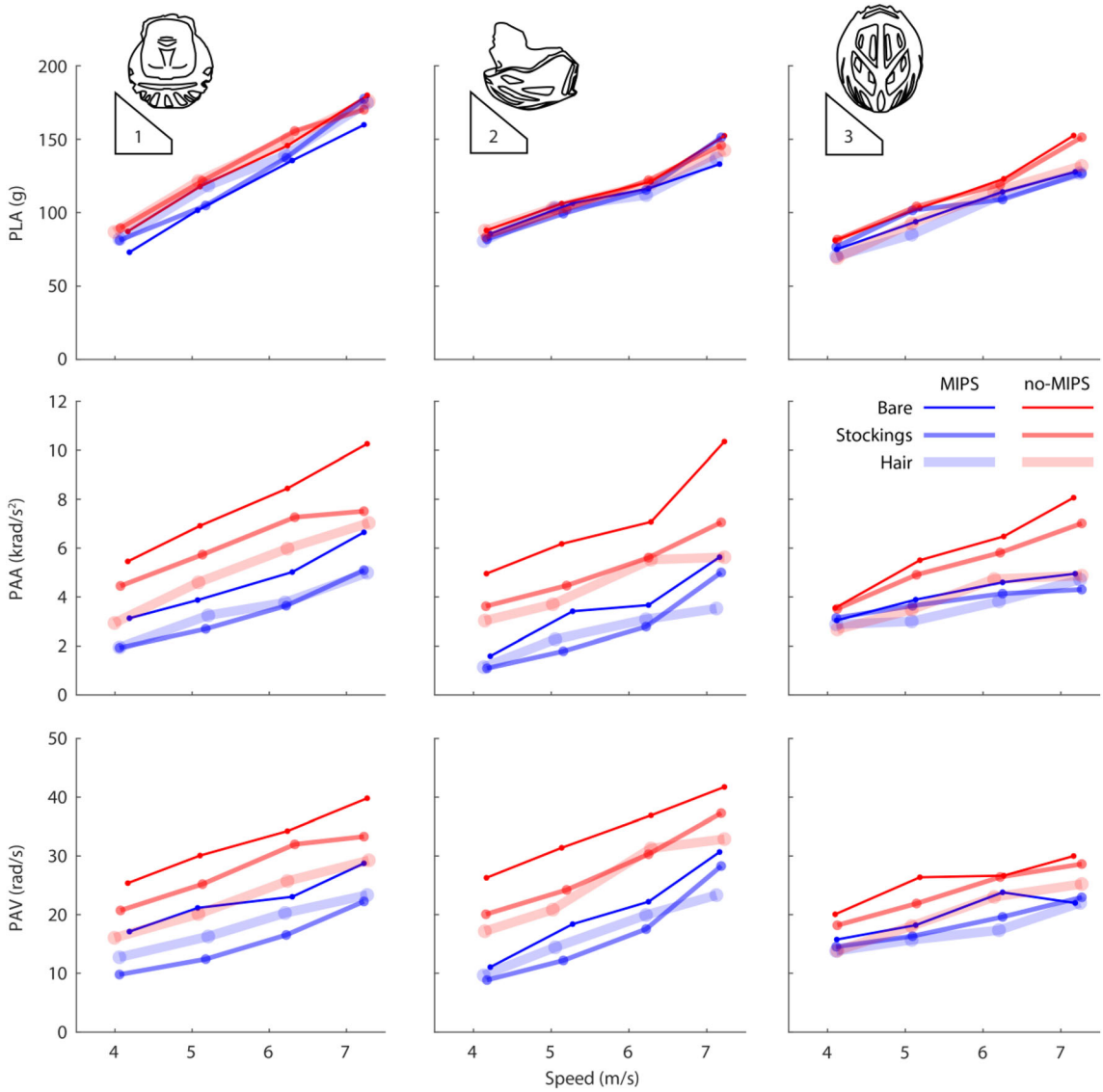


**FIGURE 3. Peak linear acceleration (PLA), peak angular acceleration (PAA), and peak angular velocity (PAV) vs. impact speed for all headform conditions (bare, stocking, hair), helmet conditions (no-MIPS, MIPS) and impact orientations (1, 2, 3).**

changes in $\Delta_{MIPS}$ with headform condition, impact orientation or impact speed.

With respect to our secondary hypotheses, the one-sample Student's t-test of the normalized data showed that angular kinematics for the bare no-MIPS conditions were significantly larger than all other conditions. (Table 3). The two-sample Student's t-test of the normalized data showed that the bare headform peak angular kinematics were attenuated more by MIPS than by hair (without MIPS), but these differences in attenuation were not significantly different (Table 3). Specifically, the normalized PAA was reduced to 0.60 by MIPS compared to 0.65 by hair ($p = 0.227$), and normalized PAV was reduced to 0.69 by MIPS compared to 0.74 by hair ($p = 0.116$). The addition of a MIPS helmet to the hair or stocking condition further attenuated both PAA (from 0.65 to 0.47; $p = 0.001$ for hair, and from 0.82 to 0.48; $p < 0.001$ for stockings) and PAV (from 0.74 to 0.57; $p < 0.001$ for hair, and from 0.86 to 0.55; $p < 0.001$ for stockings).

## DISCUSSION

This study quantified the effects of MIPS (present vs. absent) on peak headform kinematics for three headform conditions (bare, stocking-covered, and human hair wig) in three impact orientations over a range of impact speeds. Overall, MIPS lowered peak angular headform kinematics for all headform conditions, impact orientations, and impact speeds tested.

**TABLE 2. Mean and standard deviation (in parentheses) of $\Delta_{MIPS}$ (the percent reduction in peak response from the no-MIPS to MIPS conditions) for peak linear acceleration (PLA), peak angular accleration (PAA), peak angular velocity change (PAV), and brain injury criterion (BrIC) as a function of the 3 headform conditions (bare, stocking, hair), 3 impact orientations (1, 2, 3), and impact speeds.**

| | PLA | | PAA | | PAV | | BrIC | |
|---|---|---|---|---|---|---|---|---|
| Headform Condition | | | | | | | | |
| Bare | 9.3 | (4.9)[a] | 39.0 | (11.9)[a] | 32.4 | (10.46)[a] | 33.3 | (10.64)[a] |
| Stocking | 6.5 | (6.1)[ab] | 41.6 | (15.9)[a] | 36.0 | (13.36)[a] | 38.2 | (12.70)[a] |
| Hair | 3.7 | (3.1)[b] | 30.2 | (17.5)[b] | 24.4 | (11.00)[b] | 25.9 | (13.01)[b] |
| *p*-value | 0.027 | | 0.001 | | < 0.001 | | < 0.001 | |
| Impact orientation | | | | | | | | |
| 1 (*X*-rotation) | 8.4 | (5.6)[a] | 39.2 | (8.8)[a] | 33.1 | (10.9)[a] | 31.5 | (11.2)[a] |
| 2 (*Y*-rotation) | 3.4 | (3.9)[a] | 47.4 | (12.9)[b] | 38.1 | (10.6)[a] | 41.2 | (11.5)[b] |
| 3 (*ZY*-rotation) | 7.6 | (5.0)[a] | 22.9 | (14.5)[c] | 20.5 | (8.6)[b] | 23.6 | (10.0)[c] |
| *p*-value | 0.038 | | < 0.001 | | < 0.001 | | < 0.001 | |
| Impact speed | | | | | | | | |
| Coefficient[d] | 0.2 | | − 1.8 | | − 2.6 | | − 3.3 | |
| *p*-value | 0.768 | | 0.217 | | 0.019 | | 0.006 | |

Data for the headform condition are pooled across all impact orientations and speeds, and data for the orientations are pooled across all headform conditions and impact speeds. *Note* superscripts a, b, and c indicate homogeneous groups (values that share a letter are not significantly different) within each dependent variable and main effect. Superscript d: units of the coefficient are % reduction per m/s.

**TABLE 3. Mean and standard deviation (in parentheses) of the peak kinematics and BrIC normalized to the bare, no-MIPS condition**

| | PLA | | PAA | | PAV | | BrIC | |
|---|---|---|---|---|---|---|---|---|
| | no-MIPS | MIPS | no-MIPS | MIPS | no-MIPS | MIPS | no-MIPS | MIPS |
| Bare | 1 | 0.91 (0.05) | 1 | 0.60 (0.13) | 1 | 0.69 (0.12) | 1 | 0.67 (0.12) |
| Stocking | 0.99 (0.04) | 0.93 (0.05) | 0.82 (0.09) | 0.48 (0.18) | 0.86 (0.07) | 0.55 (0.15) | 0.87 (0.07) | 0.53 (0.15) |
| Hair | 0.96 (0.05) | 0.92 (0.06) | 0.65 (0.08) | 0.47 (0.15) | 0.74 (0.08) | 0.57 (0.10) | 0.73 (0.08) | 0.55 (0.10) |

Significant differences between cells are indicated by dark lines (adjacent cells) or opposing triangles (diagonal cells).

Despite this general pattern, we also observed differences in the effectiveness of MIPS across the different headform conditions, impact orientations, and to a lesser extent, impact speeds.

Headform condition influenced angular kinematics both with and without MIPS. Peak angular kinematics were largest for the no-MIPS-bare condition and smallest for the MIPS-stocking and MIPS-hair conditions. Adding a MIPS helmet to the bare headform or adding hair to the no-MIPS-bare condition reduced angular kinematics by similar amounts and adding MIPS to the hair condition reduced angular kinematics even further. These findings indicate that hair, like MIPS, adds a shear layer between the headform and helmet, but that the combination of hair and MIPS reduces headform angular kinematics more than either hair or MIPS alone. The stocking condition also adds a shear layer between the headform and helmet, and although is it less effective than hair on the bare headform, the combination of stockings and MIPS is similar to that of hair and MIPS. How to interpret these findings in the context of real-world head impacts depends on how the quantity and length of a cyclist's hair represent these headform conditions. A bare headform, stocking-covered, or somewhere between the two, may represent a bald cyclist's head. If the former, then MIPS provides bald cyclists the benefits that cyclists with hair already have without MIPS. If a stocking-covered headform, then MIPS provides a proportionally larger benefit to bald cyclists than to cyclists with a full head of hair. While further work is needed to test different types and quantities of stockings and hair and compare them to the variability of hair on human heads, our results show that a bare

headform likely overestimates the angular headform kinematics—with or without MIPS—for many actual helmet users. This phenomenon may be related to differences in the friction between the helmet and the different headform conditions and is discussed in more detail below.

The reduction in angular kinematics depended on impact orientation. Impact orientations 1, 2, and 3 were intended to generate *X*, *Y*, and *Z* headform rotations. Nearly pure *X*- and *Y*-rotations were produced at impact orientations 1 and 2, respectively, while orientation 3 produced a combined rotation, mostly about the *Z*- and *Y*- axes (Fig. S3, Supplemental Material). Other researchers have also sought to produce *Z*-axis rotations, but did not demonstrate if their rotations were purely about the *Z*-axis or some combination of axes.[39,44] Here, $\Delta_{MIPS}$ was larger for orientation 2 (*Y*-axis rotation) than for orientation 1 or 3 (*X*- or *ZY*-rotation) (Table 2, Fig. 4). MIPS's increased effectiveness during *Y*-axis rotations compared to *X*-axis rotations may be related to the larger radius of the headform and helmet in the mid-sagittal plane compared to the coronal plane. Helmet rotations in the transverse plane (i.e., about the *Z*-axis) may be limited by the interaction between the head and helmet due to their oval cross-sections. The larger radius and arc length for *Y*-axis rotations may allow the helmet to move more during the impact compared to the other axes and allow MIPS to maximize its effectiveness. Abayazid *et al.*[2] also reported that MIPS was more effective during *Y*-axis rotations compared to primarily *X*- or *Z*-axis rotations and similarly suggested this is because the helmet is less constrained to rotate during *Y*-axis rotations.

Direct interaction between the MIPS liner and the adjacent EPS liner during the impact may also explain MIPS's varying effectiveness in different impact orientations. The MIPS liner is shaped to match the helmet's ribs and vents, which are primarily oriented along the helmet's long axis (Fig. 1). During a *Y*-axis rotation, the MIPS liner slides along the helmet's ribs and thus maintains contact with the EPS. In contrast, during an *X*-axis rotation, the long, narrow sections of the MIPS liner slide across the helmet's ribs, potentially exposing the EPS to interact directly with the headform. This interaction may limit the rotation of

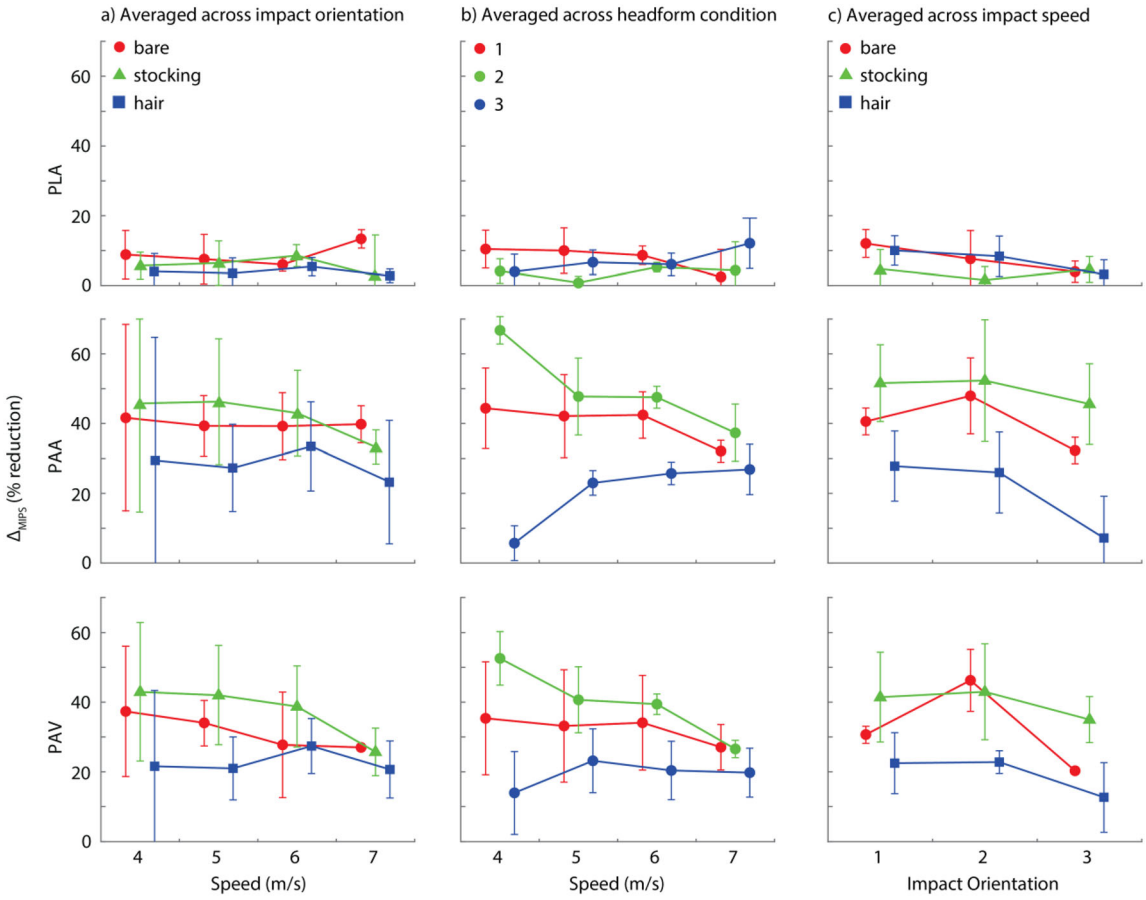


**FIGURE 4. The mean and standard deviation of $\Delta_{MIPS}$ for the peak kinematic variables averaged across (a) impact orientation; (b) headform condition, and (c) impact speeds.**

the helmet relative to the head and therefore diminish the effect of MIPS on attenuating the angular kinematics.

We also observed a third potential explanation for the orientation-specific effectiveness of MIPS. During orientations 1 and 2, MIPS reduced PAA mainly by reducing the magnitude of the *X*- and *Y*-components, respectively. However, during orientation-3 impacts, MIPS reduced PAA mainly by delaying the *Z*-axis response relative to the *Y*-axis response (Fig. S2, Supplemental Materials) and thus yielding a lower peak resultant angular acceleration. Further analysis is needed to understand how effective this alteration is in reducing actual brain strains.

Although impact speed had a large and obvious effect on the absolute magnitude of all peak kinematic responses, our analysis of the pooled data indicated that MIPS was similarly effective across all speeds (Table 2). A more detailed look at the data, however, showed that the percent reduction ($\Delta_{MIPS}$) provided by MIPS in PAA and PAV appeared to vary between the three impact orientations at the 4 m/s impact speed but became more consistent across impact orientations at the higher impact speeds (middle column, Fig. 4). The reason for this response remains unclear and additional tests are needed to better assess the importance of this interaction.

Our data supports and extends the prior work of others. Bliven *et al.*[6] also reported that MIPS had no significant effect on peak linear acceleration but significantly reduced peak angular acceleration of the head during oblique impacts. In comparison to Bliven *et al.*[6] we saw a 50% reduction in PAA and a 42% reduction in PAV for forehead impacts (orientation 2) with a stocking-covered Hybrid III headform at 6.2 m/s, whereas they reported reductions of 22 and 23%, respectively. The smaller attenuation they reported could be due to their use of a Hybrid III neck rigidly attached to a guided trolley, which alters the headform kinematics compared to a freefalling head.[11,16,18,28] Bland *et al.*[5] also performed oblique impacts to a variety of bicycle helmets with the goal of developing a rating system. We were unable to directly compare our results to theirs because they used a different headform, averaged results over multiple impact locations, combined results from both MIPS and traditional helmets, and did not compare the same helmet model with and without MIPS.

In contrast to our findings and those of others[5,6,8], Zouzias *et al.*[47] reported no significant differences in PAA and PAV between bicycle helmets with and without MIPS when placed on a Hybrid III headform partially covered by a porcine scalp and exposed to an oblique 6-m/s forehead impact that induced a y-axis rotation. While it remains unclear how well the porcine scalp represents a human scalp during a helmeted head impact, their data nonetheless show that a low-friction shear layer between the skull and scalp can attenuate and, in some cases, eliminate the beneficial effects of anti-rotation helmet systems. Further work is needed to show the biofidelity of the porcine scalp during oblique testing (e.g., coverage, shear properties, method of attachment) or to develop a realistic human scalp simulant to better assess the contribution of anti-rotation systems to head injury protection over the wide range of impact conditions that occur in the field.

Prior work has shown that differences in headform shape, surface, and moments of inertia between the Hybrid III 50th-percentile male and NOCSAE headforms can contribute to differences in angular acceleration during testing.[12,23] Our work extends these findings by showing that differences in headform conditions also need to be considered when making inter-laboratory comparisons of oblique helmet impacts. One or more layers of stockings are often used to cover the vinyl nitrile skin of the Hybrid III headform to reduce the friction between the helmet and the headform,[6–8,22,34] whereas hair has been considered less frequently during helmet testing.[7,29] Although we included a human-hair condition, the amount and length of this hair does not represent all human hair conditions and the shear properties that exist between a human scalp and the skull were missing. The effect of a scalp has been studied using a hairless porcine scalp glued to a Hybrid III headform during oblique helmet testing,[44,47] although it remains unclear how much of the reduction in angular kinematics these authors observed was the result of the headform-scalp interface vs. the scalp-helmet interface.

In the no-MIPS condition, PAA and PAV were highest for the bare headform condition, followed by the stocking condition, then the hair condition. This order may be related to differences in the coefficient of friction (CoF) of the three headform conditions. Based on the force needed to slowly pull a weighted nylon strap over a 90° arc of each headform condition, we confirmed that the bare headform had the highest CoF (1.07), followed by the stocking condition (0.26) and then the hair condition (0.17) (Fig. S4, Supplemental Materials). Trotta *et al.*,[43] evaluated the sliding properties between a helmet liner, scalp, and skull by applying a combined normal and tangential force through a fabric-covered probe against 5 post-mortem human subject (PMHS) heads. They found that scalp-skull CoF was not significantly different between the hair and shaved conditions (range 0.03–0.15) and that scalp-liner CoF was significantly different between the hair and shaved conditions (range 0.20–0.32). Differences between their and our test methods make a direct comparison difficult, although their measurement of

the Hybrid III surface friction was 0.75 compared to our 1.07. If we simply scaled our friction measurements by this ratio (0.75/1.07) for comparison purposes, then our stocking condition would scale to 0.18 and hair condition would scale to 0.12, both of which are in the realm of the CoFs they measured on the cadaver heads. These comparisons suggest that it might be possible for layers of stockings to generate a condition similar to the liner-scalp interface and that long human hair, perhaps combined with layers of stockings, might be one way to simulate the low scalp-skull frictions observed by Trotta *et al.*[43] Before considering these proposals further, more work is needed to quantify the friction of the headform conditions tested here under more realistic loading conditions and to account for the various interfaces that exist *in-vivo* between the skull and the helmet. We can then translate this knowledge into a more biofidelic headform condition to evaluate systems like MIPS that are designed to attenuate the angular kinematics of helmeted head impacts.

In this study, the effectiveness of MIPS was compared within the same helmet by removing the MIPS liner and reinstalling the comfort pads in their respective locations on the EPS liner to create the no-MIPS condition. This approach allowed us to better isolate the effect of MIPS without the confounding effects present in prior studies that used different helmet models for the MIPS and no-MIPS conditions.[8,39] However, to achieve this better isolation of MIPS performance, our study was limited to one size of one helmet model and it remains unclear how MIPS behaves in other helmet sizes and models. We also limited this study to three impact orientations and one anvil angle. Future work could consider other impact orientations, especially those the match real-world helmet impact locations[3,10,38] and a broader range of impact angles.[35,46] Finally, in order to maintain statistical power to evaluate the main effects, we did not include interaction terms in the model, but instead explored interactions graphically.

In summary, we demonstrated that MIPS reduced peak angular kinematics across 3 headform conditions, 3 impact orientations, and 4 impact speeds. Adding hair or stockings to a bare headform reduces angular kinematics and adding MIPS to a hair or stocking-covered headform further reduces the peak angular kinematics. MIPS was most effective for impacts that generated *Y*-axis rotations and, on average, yielded proportionally similar levels of attenuation across the range of speed tested here. Overall, our data reveal the importance of using a consistent headform condition when evaluating the effective of helmet systems designed to attenuate head rotations during oblique impacts.

## SUPPLEMENTARY INFORMATION

The online version contains supplementary material available at https://doi.org/10.1007/s10439-022-02961-w.

## ACKNOWLEDGMENTS

The authors would like to thank Jeff Nickel and Mircea Oala-Florescu for their assistance with the experimental set-up.

## CONFLICT OF INTEREST

All of the authors are employees of MEA Forensic Engineers & Scientists and their work may benefit from this research. Author GPS is an owner and director of MEA Forensic Engineers & Scientists. MIPS AB provided guidance in fabricating our helmet drop tower.

## REFERENCES

[1]Aare, M., and P. Halldin. A new laboratory rig for evaluating helmets subject to oblique impacts. *Traffic Inj. Prev.* 4(3):240–248, 2003. https://doi.org/10.1080/15389580309879.

[2]Abayazid, F., K. Ding, K. Zimmerman, et al. A new assessment of bicycle helmets: the brain injury mitigation effects of new technologies in oblique impacts. *Ann. Biomed. Eng.* 49:2716–2733, 2021. https://doi.org/10.1007/s10439-021-02785-0.

[3]Bland, M. L., C. McNally, J. B. Cicchino, et al. Laboratory reconstructions of bicycle helmet damage: investigation of head impacts using oblique impact and CT. *Ann. Biomed. Eng.* 2020. https://doi.org/10.1007/s10439-020-02620-y.

[4]Bland, M. L., C. McNally, and S. Rowson. Differences in impact performance of bicycle helmets during oblique impacts. *J. Biomech. Eng.* 140:091005, 2018.

[5]Bland, M. L., C. McNally, D. S. Zuby, et al. Development of the STAR evaluation system for assessing bicycle helmet protective performance. *Ann. Biomed. Eng.* 48(1):47–57, 2020. https://doi.org/10.1007/s10439-019-02330-0.

[6]Bliven, E., A. Rouhier, S. Tsai, et al. Evaluation of a novel bicycle helmet concept in oblique impact testing. *Accid. Anal. Prev.* 124:58–65, 2019. https://doi.org/10.1016/j.aap.2018.12.017.

[7]Bonin, S. J., A. L. DeMarco, and G. P. Siegmund. The effect of hair and football helmet fit on headform kinematics. International Research Council on Biomechanics of Injury Conference. Athens, Greece, September 12–14, 2018.

[8]Bottlang, M., A. Rouhier, S. Tsai, et al. Impact performance comparison of advanced bicycle helmets with dedicated rotation-damping systems. *Ann. Biomed. Eng.* 48(1):68–78, 2020. https://doi.org/10.1007/s10439-019-02328-8.

[9]Bourdet, N., C. Deck, R. P. Carriera, et al. Head impact conditions in the case of cyclist falls. *Proc. IMechE Part P: J. Sport Eng. Technol.* 226(3/4):282–289, 2012.
[10]Cameron, M., C. Finch, P. Vulcan. Protective performance of bicycle helmets introduced at the same time as the bicycle helmet wearing law in Victoria. Monash University Accident Research Center Report No. 59, 1994.
[11]Chinn B., B. Canaple, S. Derler, et al. COST 327 Motorcycle safety helmets. European Commission, Directorate General for Energy and Transport, 2001.
[12]Cobb, B. R., A. M. Zadnik, and S. Rowson. Comparative analysis of helmeted impact response of Hybrid III and National Operating Committee on Standards for Athletic Equipment headforms. *Proc. IMechE Part P: J. Sport Eng. Technol.* 230(1):50–60, 2015.
[13]Consumer Product Safety Commission. 16 CFR Part 1203. Safety Standard for Bicycle Helmets; Final Rule, 1998.
[14]Ebrahimi, I., F. Golnaraghi, and G. G. Wang. Factors influencing the oblique impact test of motorcycle helmets. *Traffic Inj. Prev.* 16:404–408, 2015. https://doi.org/10.1080/15389588.2014.937804.
[15]Fahlstedt, M., K. Baeck, P. Halldin, et al. Influence of impact velocity and angle in a detailed reconstruction of a bicycle accident. International Research Council on Biomechanics of Injury Conference. Dublin, Ireland, September 12–14, 2012.
[16]Fahlstedt, M., P. Hallidin, and S. Kleiven. The protective effect of a helmet in three bicycle accidents. *Accid Anal. Prev.* 91:135–143, 2016. https://doi.org/10.1016/j.aap.2016.02.025.
[17]Gennarelli, T. A., L. E. Thibault, and A. K. Ommaya. Pathophysiologic responses to rotational and translational accelerations of the head. *Proc. Stapp Car Crash Conf.* 720970:296–308, 1972.
[18]Ghajari, G., M. S. Peldschus, U. Galvenetto, et al. Effects of the presence of the body in helmet oblique impacts. *Accid. Anal. Prev.* 50:263–271, 2013. https://doi.org/10.1016/j.aap.2012.04.016.
[19]Gurdjian, E. S., V. L. Roberts, and L. M. Thomas. Tolerance curves of acceleration and intracranial pressure and protective index in experimental head injury. *J. Trauma.* 6(5):600–604, 1966. https://doi.org/10.1097/00005373-196609000-00005.
[20]Hansen, K., N. Dau, F. Feist, et al. Angular impact mitigation system for bicycle helmets to reduce head acceleration and risk for traumatic brain injury. *Accid. Anal. Prev.* 59:109–117, 2013. https://doi.org/10.1016/j.aap.2013.05.019.
[21]Holbourn, A. H., M. A. Edin, and D. P. Oxfd. Mechanics of head injuries. *The Lancet.* 242(6267):438–441, 1943.
[22]Jadischke, R., D. C. Viano, J. McCarthy, et al. The effects of helmet weight on Hybrid III head and neck responses by comparing unhelmeted and helmeted impacts. *J. Biomech. Eng.* 138:101008, 2016.
[23]Kendall, M., E. S. Walsh, and T. B. Hoshizaki. Comparison between Hybrid III and Hodgson-WSU headforms by linear and angular dynamic impact response. *Proc. IMechE Part P: J. Sports Eng. Technol.* 226(304):260–265, 2012.
[24]Kleiven, S. Predictors for traumatic brain injuries evaluated through accident reconstructions. *Stapp Car Crash J.* 51:81–114, 2007.
[25]Klug, C., F. Feist, E. Tomasch. Testing of bicycle helmets for preadolescents. International Research Council on Biomechanics of Injury Conference, Lyon, France, September 9-11, 2015.
[26]Lissner, H. R., M. Lebow, and F. Gaynor Evans. Experimental studies on the relation between acceleration and intracranial pressure changes in man. *J. Surg. Gyn. Obst.* 111:329–38, 1960.
[27]McIntosh, A. S., A. Lai, and E. Schilter. Bicycle helmets: head impact dynamics in helmeted and unhelmeted oblique impact tests. *Traffic Inj. Prev.* 14:501–508, 2013. https://doi.org/10.1080/15389588.2012.727217.
[28]Meng, S., A. Cernicchi, S. Kleiven, et al. The biomechanical differences of shock absorption test methods in the US and European helmet standards. *Int. J. Crashworthiness.* 24(4):399–412, 2019. https://doi.org/10.1080/13588265.2018.1464545.
[29]Mills, N. J., and A. Gilchrist. Oblique impact testing of bicycle helmets. *Int. J. Impact Eng.* 35:1075–1086, 2008. https://doi.org/10.1016/J.IJIMPENG.2007.05.005.
[30]Nahum, A. M., R. Smith, C. C. Ward. Intracranial pressure dynamics during head impact. Proceedings of the 21st Stapp Car Crash Conf. 770922:339–366, 1977.
[31]Newman, J. A., M. C. Beusenberg, N. Schewchenko, et al. Verification of biomechanical methods employed in a comprehensive study of mild traumatic brain injury and the effectiveness of American football helmets. *J. Biomech.* 38:1469–1481, 2005. https://doi.org/10.1016/j.jbiomech.2004.06.025.
[32]Ommaya, K. A., and A. E. Hirsch. Tolerances for cerebral concussion from head impact and whiplash in primates. *J. Biomech.* 4:13–21, 1971. https://doi.org/10.1016/0021-9290(71)90011-x.
[33]Padgaonkar, A. J., K. W. Krieger, and A. I. King. Measurement of angular acceleration of a rigid body using linear accelerometers. *J. Appl. Mech.* 42(3):552–556, 1975.
[34]Pellman, E. J., D. C. Viano, A. M. Tucker, et al. Concussion in professional football—reconstruction of game impacts and injuries. *Neurosurgery.* 53(4):799–814, 2003. https://doi.org/10.1093/neurosurgery/53.3.799.
[35]Peng, Y., Y. Chen, J. Yang, et al. A study of pedestrian and bicyclist exposure to head injury in passenger car collisions based on accident data and simulations. *Saf. Sci.* 50:1749–1759, 2012. https://doi.org/10.1016/J.SSCI.2012.03.005.
[36]Rice, S., M. A. Iaccarino, S. Bhatnager, et al. Reporting of concussion-like symptoms after cycling crashes. *J. Athletic Train.* 55(1):11–16, 2020. https://doi.org/10.4085/1062-6050-91-19.
[37]SAE International. Instrumentation for Impact Test—Part 1—Electronic Instrumentation, J211/1_201403, 2014.
[38]Smith, T. A., D. Tees, D. R. Thom, et al. Evaluation and replication of impact damage to bicycle helmets. *Accid. Anal. Prev.* 26(6):795–802, 1994. https://doi.org/10.1016/0001-4575(94)90055-8.
[39]Stigson, H., M. Rizzi, A. Ydenius, et al. Consumer testing of bicycle helmets. International Research Council on the Biomechanics of Injury Conference, Antwerp, Belgium, September 13–15, 2017.
[40]Strich, S. J., and D. M. Oxon. Shearing of nerve fibers as a cause of brain damage due to head injury. *Lancet.* 26:443–8, 1961. https://doi.org/10.1016/S0140-6736(61)92426-6.
[41]Takhounts, E. G., M. J. Craig, K. Moorhouse, et al. Development of brain injury criteria (BrIC). *Stapp Car Crash J.* 57:243–266, 2013.
[42]Thomas, L. M., V. L. Roberts, and E. S. Gurdjian. Experimental intracranial pressure gradients in the human skull. *J. Neurol. Neurosurg. Psychiat.* 29:404–412, 1966. https://doi.org/10.1136/jnnp.29.5.404.

[43]Trotta, A., A. Annaidh, R. Burek, et al. Evaluation of the head-helmet sliding properties in an impact test. *J. Biomech*. 75:28–34, 2018. https://doi.org/10.1016/j.jbiomech.2018.05.003.
[44]Trotta, A., D. Zouzias, G. D. Bruyne, et al. The importance of the scalp in head impact kinematics. *Ann. Biomed. Eng*. 46:831–840, 2018. https://doi.org/10.1007/s10439-018-2003-0.
[45]Unterharnscheidt, F. J., L. S. Higgins. Neuropathological effects transitional and rotational accel of the head in animal experiments. in: The late effect of head injury. C. C. Thomas, 17:158–67, 1969.
[46]Verschueren, P. Biomechanical analysis of head injuries related to bicycle accidents and a new bicycle helmet concept. Katholieke Universiteit Leuven, PhD Thesis, 2009.
[47]Zouzias, D., G. D. Bruyne, A. N. Annaidh, et al. The effect of the scalp on effectiveness of bicycle helmets' anti-rotation acceleration technology. *Traffic Inj. Prev*. 22(1):51–56, 2021. https://doi.org/10.1080/15389588.2020.1841179.